Optimal and Reduced Complexity Receivers for M-ary Multi-h CPM

Erik Perrins and Michael Rice
Department of Electrical and Computer Engineering
Brigham Young University
Provo, UT 84602
Email: esp@ee.byu.edu, mdr@ee.byu.edu

***Abstract*— We present an optimal maximum likelihood sequence estimating (MLSE) receiver which is based on the pulse amplitude modulation (PAM) representation of multilevel multi-h continuous phase modulation (CPM). We also give four different approaches to constructing suboptimal receivers which use a significantly reduced number of signal terms. We apply these techniques to two multi-h schemes in current use and evaluate receiver performance with computer simulations. In one instance we reduce the number of trellis states from 512 to 32, and the number of matched filters from 96 to 3, with a degradation of 0.7 dB. The simulations also show that the complexity reductions preserve the performance advantage multi-h CPM schemes have over single-index schemes.**

I. Introduction

Continuous Phase Modulation (CPM) is advantageous for its efficient use of power and bandwidth. It also has a constant signal envelope, which is essential in applications using nonlinear amplifiers. However, it suffers from high implementation complexity and synchronization problems. In particular, those CPM schemes with efficient power and spectral properties are often the ones with higher complexity, as is the case with multi-h CPM. The optimal MLSE receiver is implemented via the Viterbi Algorithm (VA) and contains pM^{L-1} states and $N_h \cdot M^L$ correlators (matched filters), where p is the number of phase states, M is the alphabet size, N_h is the number of modulation indexes, and L is the duration of the phase pulse in symbol times. There have been a number of approaches taken to reduce both the size of the trellis and the size of the matched filter bank [1], [2].

In this paper we present a new optimal MLSE receiver for multi-h CPM which is based on the PAM representation in [3]. The receiver is a generalization of the one derived by Kaleh [4], and operates on the same trellis as the existing optimal receiver in [1]. One of the important features of the PAM decomposition is that most of the energy is concentrated in a few signal terms. These signal terms are also the ones which can be described by the smallest trellis. We exploit this characteristic and propose four approximations which reduce receiver complexity. The first two reduce the number of signal terms by using the minimum mean-squared error approximation presented in [3], [5], [6]. The third approximation divides the remaining signal terms into sets with common pulse duration and represents each set with a single averaged pulse. The last approximation reduces the trellis size with reduced state sequence estimation as proposed in [2]. These techniques are applied to two multi-h schemes known to be in use [7], [8]. For the particularly complex scheme in [8] we reduce the number of trellis states from 512 to 32, and the number of matched filters from 2×48 to 3, with a degradation of 0.7 dB as evaluated by computer simulations. The simulations also show that the complexity reduction techniques preserve the performance advantage multi-h CPM schemes have over single-index schemes. These performance gains are lost by some reduced-complexity receivers [1], [9].

In the next section we summarize the multi-h CPM signal model. In Section III we review the PAM signal model. We derive the optimal MLSE receiver in Section IV and its approximations in Section V. We give some simulation results in Section VI and give conclusions in Section VII.

II. Multi-h CPM Signal Model

The complex-baseband multi-h CPM signal is given by

$$s(t,\boldsymbol{\alpha}) = \exp\big(j\psi(t,\boldsymbol{\alpha})\big) \quad (1)$$

$$\psi(t,\boldsymbol{\alpha}) = 2\pi \sum_{i=-\infty}^{n} \alpha_i h_{\underline{i}} q(t-iT) \quad (2)$$

where T is the symbol duration, $nT \le t < (n+1)T$, $h_{\underline{i}}$ are the set of N_h modulation indexes, $\boldsymbol{\alpha} = \{\alpha_i\}$ are the information symbols in the M-ary alphabet $\{\pm 1, \pm 3, \cdots, \pm(M-1)\}$, and $q(t)$ is the phase pulse. In this paper, the underlined subscript notation in (2) is defined as modulo-N_h, i.e. $\underline{i} \triangleq i \bmod N_h$.

The phase pulse $q(t)$ and the frequency pulse $f(t)$ are related by

$$q(t) = \int_0^t f(\tau)\, d\tau. \quad (3)$$

The frequency pulse is supported over the time interval $(0, LT)$ and is subject to the constraints

$$f(t) = f(LT-t), \qquad \int_0^{LT} f(\tau)\, d\tau = q(LT) = \frac{1}{2}. \quad (4)$$

In light of the constraints on $f(t)$ and $q(t)$, Equation (2) can be written as

$$\psi(t,\boldsymbol{\alpha}) = \theta(t,\boldsymbol{\alpha}_n) + \theta_{n-L} \quad (5)$$
$$= 2\pi \sum_{i=n-L+1}^{n} \alpha_i h_{\underline{i}} q(t-iT) + \left(\pi \sum_{i=-\infty}^{n-L} \alpha_i h_{\underline{i}}\right) \bmod 2\pi.$$

 0-7803-8344-3/04/$20.00 © 2004 IEEE

TABLE I

VALUES OF $\beta_{k,i}$ AND D_k FOR THE BINARY $L = 3$ CASE

k	$\beta_{k,2}$	$\beta_{k,1}$	$\beta_{k,0}$	D_k
0	0	0	0	4
1	0	1	0	2
2	1	0	0	1
3	1	1	0	1

The term $\theta(t, \boldsymbol{\alpha}_n)$ is a function of the L symbols being modulated by the phase pulse. For $h_{\underline{i}} = 2k_{\underline{i}}/p$ ($k_{\underline{i}}$, p integers), the phase state θ_{n-L} takes on p distinct values. The signal is described by a trellis containing pM^{L-1} states, with M branches at each state. Each branch is defined by the $(L+1)$-tuple $\sigma_n = (\theta_{n-L}, \alpha_{n-L+1}, \alpha_{n-L+2}, \ldots, \alpha_n)$.

III. PAM SIGNAL MODEL FOR M-ARY MULTI-h CPM

In this section we summarize the PAM representation of multi-h CPM presented in [3]. This is a generalization of earlier work which considered the binary single-h [5] and M-ary single-h [6] cases. The derivation is lengthy so only those parts which are essential to the receiver design are summarized here. The multi-h waveform is exactly represented by

$$s(t, \boldsymbol{\alpha}) = \sum_{k=0}^{N-1} \sum_{n} a_{k,n} g_{k,\underline{n}}(t - nT) \tag{6}$$

where the signal is a sum of pulses $g_{k,\underline{n}}(t)$ scaled by the pseudo-symbols $a_{k,n}$. The important difference from the single-h case is that for each value of k, $0 \le k \le N-1$, we have $\{g_{k,\underline{n}}(t)\} = \{g_{k,\underline{0}}(t), g_{k,\underline{1}}(t), \cdots, g_{k,\underline{N_h-1}}(t)\}$. Thus we need $N_h \cdot N$ pulses to exactly represent the signal. The right-hand side of (6) applies to both binary and M-ary signaling; however, in this section we must distinguish between the binary and M-ary cases. For the sake of clarity, we label binary pseudo-symbols and pulses as $b_{k,n}$ and $c_{k,\underline{n}}(t)$ ($0 \le k \le Q-1$), and M-ary pseudo-symbols and pulses as $a_{k,n}$ and $g_{k,\underline{n}}(t)$ ($0 \le k \le N-1$). We also label binary data symbols as γ_n and M-ary data symbols as α_n.

For the binary case we obtain the pseudo-symbols from the binary information symbols γ_n according to the nonlinear mapping

$$b_{k,n} = \exp\left\{ j\pi \left[\sum_{m=-\infty}^{n} h_{\underline{m}} \gamma_m - \sum_{i=0}^{L-1} h_{\underline{n-i}} \gamma_{n-i} \beta_{k,\,i} \right] \right\} \tag{7}$$

where $0 \le k \le Q-1$ and $Q = 2^{L-1}$. Equation (7) shows that the scaled binary data symbols $h_{\underline{n}}\gamma_n$ are fed into a summing filter and into a bank of FIR filters (indexed by k). The output of the k-th FIR filter is subtracted from the output of the summing filter, forming the exponent of the non-linearity $\exp\{j\pi(\cdot)\}$. The bank of FIR filters have taps given by the radix-2 decomposition of the index k

$$k = \sum_{i=1}^{L-1} 2^{i-1} \beta_{k,i}, \qquad 0 \le k \le Q-1, \tag{8}$$

where $\beta_{k,0}$ is always zero. Table I gives the coefficients $\{\beta_{k,i}\}$ for the $L = 3$ case.

The signal pulses for the binary case, $c_{k,\underline{n}}(t)$, are a function of the phase pulse and modulation indexes and the details of their construction are presented in [3]. The pulses have a duration of

$$D_k = \min_i \big\{ L(2 - \beta_{k,i}) - i \big\}, \qquad 0 \le i \le L-1. \tag{9}$$

We now make an important point, which was observed by Kaleh [4]. For the $L = 3$ case, we note that for any index n the signal is described by the 4-tuple $\sigma_n = (\theta_{n-3}, \gamma_{n-2}, \gamma_{n-1}, \gamma_n)$, for which there are $p2^3$ distinct values. However, from (7) and Table I we see that $b_{1,n} = e^{j\theta_{n-2}} e^{j\pi h_{\underline{n}} \gamma_n}$, which is a function of the 3-tuple $(\theta_{n-2}, \gamma_{n-1}, \gamma_n)$. If this exercise is repeated for $k = 0, 1, \cdots, Q-1$ and for any value of L, it can be shown that each signal component $b_{k,n}$ is fully described by an $(L + 2 - D_k)$-tuple; thus, the longest pulses correspond to the pseudo-symbols which require the fewest states.

For M-ary signaling, Mengali [6] showed that the waveform can be viewed as the product of P binary signals, where P satisfies $2^{P-1} < M \le 2^P$. The product is formed by representing the M-ary data symbols α_i as the sum of binary data symbols $\gamma_{i,l}$

$$\alpha_i = \sum_{l=0}^{P-1} \gamma_{i,l} 2^l, \qquad \gamma_{i,l} \in \{\pm 1\}. \tag{10}$$

and then inserting (10) into (1). In Table II we show the values of $\gamma_{i,l}$ in (10) for the $M = 4$ case. The binary PAM decomposition is then applied to each of these binary subsystems. The expansion of the product of P binary signals yields (6), where $N = Q^P(2^P - 1)$. The remainder of the details are in [3], [6].

TABLE II

MAPPING FROM α_i TO $\gamma_{i,l}$ FOR THE $M = 4$ CASE

α_n	$\gamma_{n,1}$	$\gamma_{n,0}$
-3	-1	-1
-1	-1	1
1	1	-1
3	1	1

TABLE III

SIGNAL TERMS $a_{k,n}$ AND $g_{k,\underline{n}}$ FOR THE $M = 4$, $L = 3$ CASE

k	$g_{k,\underline{n}}(t)$	$a_{k,n}$	D_k
0	$c^{(0)}_{0,\underline{n}}(t) c^{(1)}_{0,\underline{n}}(t)$	$b^{(0)}_{0,n} b^{(1)}_{0,n}$	4
1	$c^{(0)}_{0,\underline{n-1}}(t+T) c^{(1)}_{0,\underline{n}}(t)$	$b^{(0)}_{0,n-1} b^{(1)}_{0,n}$	3
2	$c^{(0)}_{0,\underline{n}}(t) c^{(1)}_{0,\underline{n-1}}(t+T)$	$b^{(0)}_{0,n} b^{(1)}_{0,n-1}$	3
3	$c^{(0)}_{0,\underline{n-2}}(t+2T) c^{(1)}_{0,\underline{n}}(t)$	$b^{(0)}_{0,n-2} b^{(1)}_{0,n}$	2
.	.	.	.
.	.	.	.
47	$c^{(0)}_{3,\underline{n}}(t) c^{(1)}_{3,\underline{n}}(t)$	$b^{(0)}_{3,n} b^{(1)}_{3,n}$	1

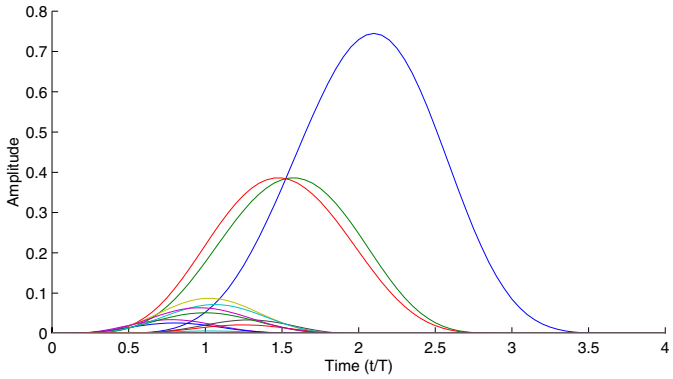

Fig. 1. The 48 signal pulses $g_{k,0}(t)$ for $M = 4$, $h = \{4/16, 5/16\}$, $L = 3RC$, n-even

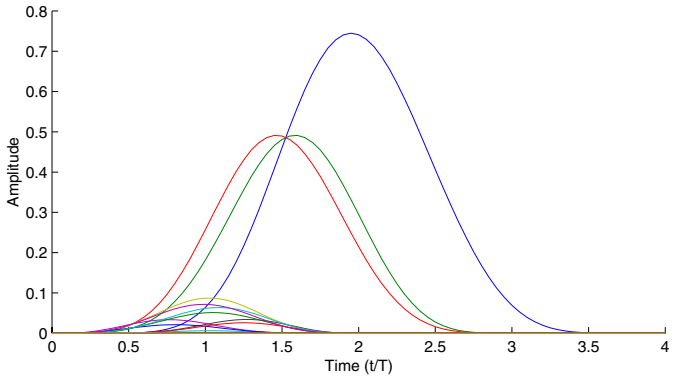

Fig. 2. The 48 signal pulses $g_{k,1}(t)$ for $M = 4$, $h = \{4/16, 5/16\}$, $L = 3RC$, n-odd

For the purposes of this paper, it is important to know that each M-ary signal element ($a_{k,n}$ or $g_{k,\underline{n}}(t)$) is the product of P binary signal elements ($b_{k,n}$ or $c_{k,\underline{n}}(t)$). For example, when $M = 4$ and $L = 3$ the PAM representation has $N = 48$ terms, each term being a product of $P = 2$ binary terms. Table III shows a few of these 48 signal terms. From Table III we see that $a_{3,n} = b^{(0)}_{0,n-2} b^{(1)}_{0,n}$. We obtain $b^{(l)}_{k,n}$ from (7) by replacing $h_{\underline{n}}$ with $h^{(l)}_{\underline{n}} = 2^l h_{\underline{n}}$. We can see from (7) that $a_{3,n}$ is a function of the 3-tuple $(\theta_{n-2}, \alpha_{n-1}, \alpha_n)$. Thus, it can also be shown for the M-ary case that each signal element $a_{k,n}$ is a function of an $(L + 2 - D_k)$-tuple. The exception to this rule (for both binary and M-ary cases) is $a_{0,n} = a_{0,n-1} e^{j\pi h_{\underline{n}} \alpha_n}$ which is described by a 2-tuple [4]. We can group the signal elements with a common pulse duration in to sets defined by

$$\mathcal{K}_j = \{k : D_k = L + 1 - j\}, \qquad 0 \le j \le L. \tag{11}$$

where $\mathcal{K}_0$ contains the most significant pulse, etc.

Figures 1 and 2 show the 2 sets of $N = 48$ pulses for the case where $M = 4$, $h = \{4/16, 5/16\}$, $L = 3RC$. The set $\mathcal{K}_0$ has one pulse with duration $4T$, and $\mathcal{K}_1$ has 2 pulses with duration $3T$. In $\mathcal{K}_2$ there are 9 small pulses of duration $2T$, and the 36 length-T pulses in $\mathcal{K}_3$ are not visible in the figures.

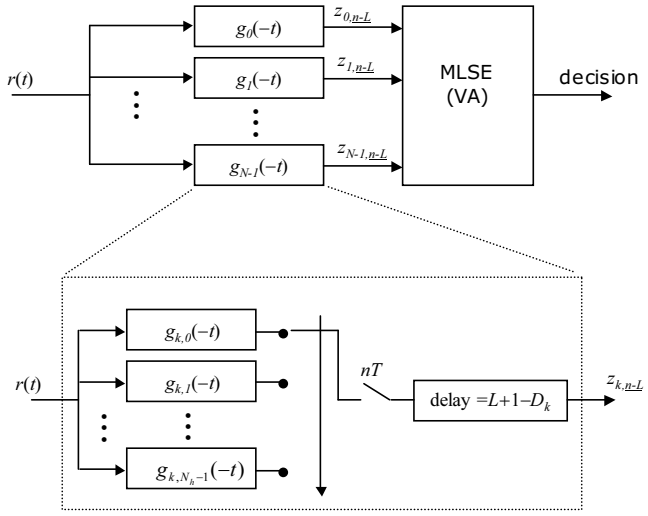

Fig. 3. MLSE receiver structure with expanded view of multi-h matched filter and delay

IV. Optimal Receiver

The MLSE receiver for the equivalent PAM representation was derived by Kaleh [4], and requires only trivial extension to accommodate the multi-h case. The complex-baseband received signal model is

$$r(t) = s(t, \boldsymbol{\alpha}) + n(t) \tag{12}$$

where $n(t)$ is additive white Gaussian noise (AWGN) with one-sided power spectral density N_0. Due to the AWGN assumption, the receiver selects as its output the information sequence $\tilde{\boldsymbol{\alpha}}$ which minimizes the Euclidian distance

$$\lambda(\tilde{\boldsymbol{\alpha}}) = \int_{-\infty}^{\infty} |r(t) - s(t, \tilde{\boldsymbol{\alpha}})|^2 \, dt. \tag{13}$$

Since $s(t, \boldsymbol{\alpha})$ is constant envelope, minimizing (13) is equivalent to maximizing the correlation

$$\lambda(\tilde{\boldsymbol{\alpha}}) = \mathrm{Re} \int_{-\infty}^{\infty} r(t) s^*(t, \tilde{\boldsymbol{\alpha}}) \, dt. \tag{14}$$

We insert (6) into (14) and with some reordering of terms arrive at the recursive branch metric

$$\lambda_i(n) = \lambda_i(n-1) + \mathrm{Re} \sum_{k=0}^{N-1} z_{k,\underline{n}} a^{*i}_{k,\underline{n}} \tag{15}$$

$$z_{k,\underline{n}} = \int_{nT}^{(n+D_k)T} r(t) g_{k,\underline{n}}(t - nT) \, dt \tag{16}$$

where the i-th branch in the trellis has an $(L + 1)$-tuple associated with it, and a corresponding set of N pseudo-symbols $a^i_{k,\underline{n}}$. Practically speaking, the limits of integration in (16) mean that the sampled matched filter outputs $z_{k,\underline{n}}$ are computed with a delay of L symbol intervals, since $\max\{D_k\} = L + 1$.

The structure of the receiver is shown in Figure 3. The received signal $r(t)$ is fed into the bank of $N_h \cdot N$ matched

filters. The sampled filter outputs are the inputs to the VA, which computes branch metrics, determines the surviving path at each merging node, and outputs a decision. The figure also shows an expanded view of the k-th filter in the bank. Each filter actually consists of a set of N_h filters whose sampled outputs are cyclically selected using a commutator and then delayed by the amount needed to have an overall filter delay of L symbol times.

It is interesting to note that this receiver requires a bank of $N_h \cdot N$ matched filters ($N = Q^P(2^P - 1)$) whose impulse responses range in duration from T to $(L+1)T$. The total number of length-T segments in the filter bank is $N_h \cdot M^L$, which is identical to the number required by the receiver in [1]. Thus, there is no complexity savings offered by the receiver presented above. We have simply "reorganized" the matched filter bank to contain filters of varying lengths. We will now exploit this reorganization to obtain a number of complexity reductions.

V. Reduced Complexity Receivers

Approximation #1: Reducing the trellis size

This approximation was proposed by Kaleh [4]. We simply exploit the fact that not all signal terms in the PAM representation require the full trellis described by the $(L+1)$-tuple. The approximate signal is given by

$$\hat{s}(t, \boldsymbol{\alpha}) = \sum_{k \in \mathcal{K}} \sum_{n} a_{k,n} p_{k,\underline{n}}(t - nT) \tag{17}$$

where $\mathcal{K}$ is a subset of $\{0, 1, 2, \cdots, N-1\}$ with the number of elements given by $|\mathcal{K}|$. A natural choice is to select $\mathcal{K}$ in terms of $\mathcal{K}_j$, since the trellis size grows incrementally larger with j, i.e. the number of states is pM^{j-1} for $1 \le j \le L$. For example, Mengali [6] proposed $\mathcal{K} = \mathcal{K}_0 + \mathcal{K}_1$, which corresponds to a trellis with p states.

The signal pulses $p_{k,\underline{n}}(t)$ in (17) are the minimum mean-squared error approximation to the signal, which is described in [3], [5], [6]. Since (17) is no longer constant envelope, minimizing (13) is equivalent to maximizing

$$\lambda(\tilde{\boldsymbol{\alpha}}) = \mathrm{Re} \int_{-\infty}^{\infty} r(t) \hat{s}^*(t, \tilde{\boldsymbol{\alpha}})\, dt - \frac{1}{2} \int_{-\infty}^{\infty} |\hat{s}(t, \tilde{\boldsymbol{\alpha}})|^2\, dt \tag{18}$$

The first term in (18) is similar to that in (15), and is a function of a reduced $(L+2-\min_{\mathcal{K}}\{D_k\})$-tuple; however, the second term in (18) remains a function of the original $(L+1)$-tuple. To overcome this problem, we will use the concept of decision feedback. Each state in the reduced trellis maintains a record of recent merge decisions. These recent decisions are used to fill out the original $(L+1)$-tuple. It has been shown in [2] that decision feedback can be used in many instances without any loss in performance. This leads to the recursive metric

$$\lambda_i(n) = \lambda_i(n-1) + \mathrm{Re} \sum_{k \in \mathcal{K}} z_{k,\underline{n}} a^{*i}_{k,\underline{n}} - S^i \tag{19}$$

$$S^i = \frac{1}{2} \int_0^T \Big| \sum_{k \in \mathcal{K}} \sum_{n} a^{(d_i,i)}_{k,n} p_{k,\underline{n}}(t - nT) \Big|^2\, dt \tag{20}$$

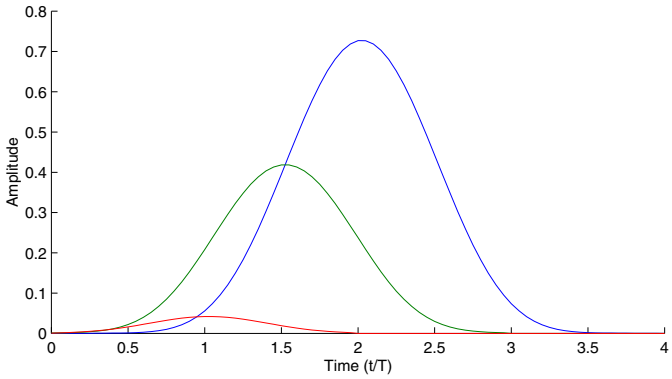

Fig. 4. Three pulses $p_{\mathcal{K}_0}(t)$, $p_{\mathcal{K}_1}(t)$, and $p_{\mathcal{K}_2}(t)$ for the 4-ary $3RC$, $h = \{4/16, 5/16\}$ case.

where $z_{k,\underline{n}}$ is as defined in (16) except $g_{k,\underline{n}}(t)$ is replaced with $p_{k,\underline{n}}(t)$. The record of recent decisions along the i-th branch is denoted by d_i and the concatenation of (d_i, i) in (20) forms an $(L+1)$-tuple. If (17) is very close to being constant envelope then S^i can be ignored, as was the case in [4]; however, for multi-h schemes, ignoring S^i can produce significant performance degradations.

The i-th branch in this trellis has an $(L+2-\min_{\mathcal{K}}\{D_k\})$-tuple associated with it. The receiver requires a bank of $N_h \cdot |\mathcal{K}|$ matched filters.

Approximation #2: Reducing the matched filter bank by N_h

This approximation is proposed for the first time in this paper, since it is specific to multi-h schemes. We can approximate the set of pulses $\{g_{k,\underline{n}}(t)\} = \{g_{k,\underline{0}}(t), g_{k,\underline{1}}(t), \cdots, g_{k,\underline{N_h-1}}(t)\}$ with a single pulse $p_k(t)$ by averaging over the modulation indexes using the minimum mean-squared error approximation in [3]. While this can be done for all values of modulation indexes, it can be shown [3] that it is most practical when

$$\max_i \{2^{P-1} h_i\} \le \frac{1}{2} \tag{21}$$

is satisfied. This approximation reduces the filter-commutator-delay structure in Figure 3 to a single filter $p_k(-t)$ followed by the delay element, which reduces the overall number of matched filters by a factor of N_h. The metric for this approximation is

$$\lambda_i(n) = \lambda_i(n-1) + \mathrm{Re} \sum_{k \in \mathcal{K}} z_{k,n} a^{*i}_{k,\underline{n}} - \bar{S}^i \tag{22}$$

where $\bar{S}^i$ is computed with (20) by replacing $p_{k,\underline{n}}(t)$ with $p_k(t)$. Here the structure of the matched filter bank is identical to that of a single-h receiver since the matched filter outputs $z_{k,n}$ are no longer selected in a modulo-N_h fashion. It is important to note that the trellis remains unchanged. In Section VI we show that this approximation preserves the gains that multi-h schemes have over single-h schemes.

Approximation #3: Averaging the pulses over $\mathcal{K}_j$

The underlying concept of this approximation was originally outlined in [10]. In many instances, the pulses in the sets $\mathcal{K}_j$

are very similar to each other. Thus, we can approximate all the pulses in the set $\mathcal{K}_j$ by a single averaged pulse, $p_{\mathcal{K}_j}(t)$. For example, in Figures 1 and 2 we see one pulse in $\mathcal{K}_0$, two pulses in $\mathcal{K}_1$, and nine pulses in $\mathcal{K}_2$. We can average the pulses within these three sets to obtain the pulses shown in Figure 4.

We then find the coefficient d_k which minimizes the mean-squared error between each pulse in the set and the averaged pulse, i.e.

$$d_k = \arg\min_d \int_0^{D_k T} \left(d \cdot p_{\mathcal{K}_j}(t) - p_k(t)\right)^2 \, dt. \tag{23}$$

This scale factor can be applied offline to the pseudo-symbols in the set

$$a^i_{\mathcal{K}_j,\underline{n}} = \sum_{k \in \mathcal{K}_j} d_k a^i_{k,\underline{n}} \tag{24}$$

so there is a one-to-one correspondence between pulses $p_{\mathcal{K}_j}(t)$ and pseudo-symbols $a^i_{\mathcal{K}_j,\underline{n}}$. The metric in this case is

$$\lambda_i(n) = \lambda_i(n-1) + \mathrm{Re} \sum_j z_{\mathcal{K}_j,n} a^{*i}_{\mathcal{K}_j,\underline{n}} - \bar{S}^i. \tag{25}$$

From the discussion in Approximation #1 we see that each additional filter $p_{\mathcal{K}_j}(t)$, $1 \le j \le L$, requires a factor of M increase in the size of the trellis. Thus we have a one-to-one correspondence in the number of matched filters and the increments in the trellis size. In Section VI we show that while some of these pulses are small, as seen in Figure 4, their impact on receiver performance can be very noticeable.

Approximation #4: Reduced state sequence estimation

The last approximation was proposed by Svensson [2] for partial response CPM; however, it has not been examined in the context of the PAM decomposition. There are two approaches in this approximation. The first removes symbols from the $(L+1)$-tuple and replaces them with decision feedback For example, when $L = 2$ we have a trellis defined by the 3-tuple $\sigma_n = (\theta_{n-2}, \alpha_{n-1}\alpha_n)$ for which there are pM states. If we approximate α_{n-1} with $\hat{\alpha}_{n-1}$, where $\hat{\alpha}_{n-1}$ is the symbol associated with the surviving branch at the previous merge, then we do not have to account for α_{n-1} with a larger trellis. We reduce the number of states by a factor of M. In general, we force the trellis to have an effective correlative memory of L', where $1 \le L' < L$. The drawback is that this usually shortens the length of time in which competing signals are kept separate within the trellis and thus lowers the distance accumulated between those signals; however, we have seen that Approximation #1 allows a natural means of removing symbols from the $(L+1)$-tuple by simply discarding the least significant signal terms. For this reason we will select Approximation #1 over this option when possible.

The second option with this approximation is to reduce the number of phase states. We pursue this option in this paper because it can often be applied with little or no effect on performance [2]. We simply maintain a trellis with a smaller number of phase states, p', where $1 \le p' < p$ (for simplicity, we concentrate on the special case where p' divides p evenly). For the purposes of the trellis, the original p phase states have

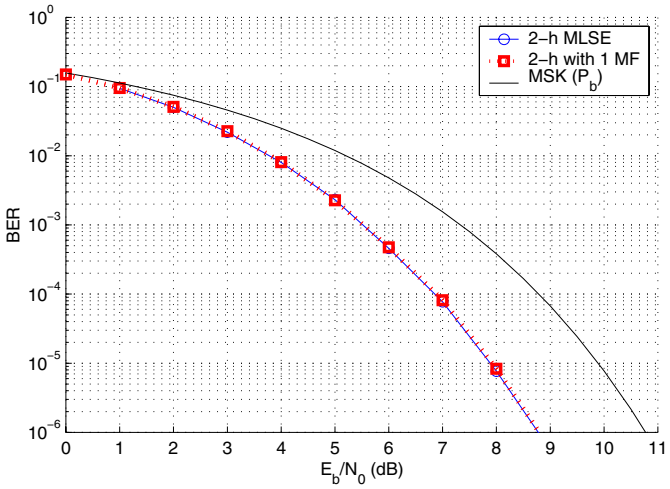

Fig. 5. Performance of binary $1REC$ with $h = \{3/8, 4/8\}$. The simulations do not show any loss relative to MLSE when using Approximation #2 (2 matched filters vs. 1). The solid line is for the optimal receiver, the dotted line is for the simplified receiver. Multi-h performance gains are preserved over single-h MSK.

indexes in the range $0 \le i_\theta \le p-1$. The trellis paths that occupy these states conform to

$$i_\theta = \left(\sum_{i=-\infty}^{n-L} \alpha_i k_{\underline{i}} \right) \bmod p \tag{26}$$

as we see from (5). We simply redefine the index as

$$i_{\theta'} = i_\theta \bmod p' = \left(\sum_{i=-\infty}^{n-L} \alpha_i k_{\underline{i}} \right) \bmod p'. \tag{27}$$

However, to compute the branch metrics in (15) we must have the original phase state index which we compute directly from (26) using decision feedback to approximate the symbols α_n. These concepts are explained in greater detail in [2].

VI. Simulation Results

Binary $1REC$ with $h = \{3/8, 4/8\}$

We first consider the binary $L = 1REC$ case with $h = \{3/8, 4/8\}$. This is a commonly used example [11], [12] and is also part of the satellite communication standard MIL-STD-188-181B [7]. The optimal receiver consists of a bank of two matched filters, $g_{0,\underline{0}}(-t)$ and $g_{0,\underline{1}}(-t)$, and a $pM^{L-1} = 16$ state trellis. Since this is a full response CPM scheme, the only approximation we apply is to average the pulses over the modulation indexes (Approximation #2). The simulation results in Figure 5 show this simplification has no observable loss relative to MLSE. (the solid and dotted lines are essentially on top of one another). The figure also shows the known 2 dB performance gain this multi-h scheme has over MSK ($1REC$, $h = 1/2$, 4-state trellis). For the MLSE receiver, the multi-h gain over MSK is achieved by the increased size of the trellis (16 states vs. 4), and the larger filter bank (2 filters vs. 1). For the simplified receiver, only the trellis size is larger while the performance gains are entirely preserved.

TABLE IV

TWO REDUCED-COMPLEXITY RECEIVERS OF 16-STATES AND 32-STATES FOR $M = 4$, $3RC$ WITH $h = \{4/16, 5/16\}$.

	States	Filters	Loss
MLSE	512	$2 \cdot 48$	0
#1	32	$2 \cdot 3$	1.6
#2	32	3	2.6
#3	32	2	2.6
#4	16	2	2.6

	States	Filters	Loss
MLSE	512	$2 \cdot 48$	0
#1	128	$2 \cdot 12$	0
#2	128	12	0.1
#3	128	3	0.2
#4	32	3	0.7

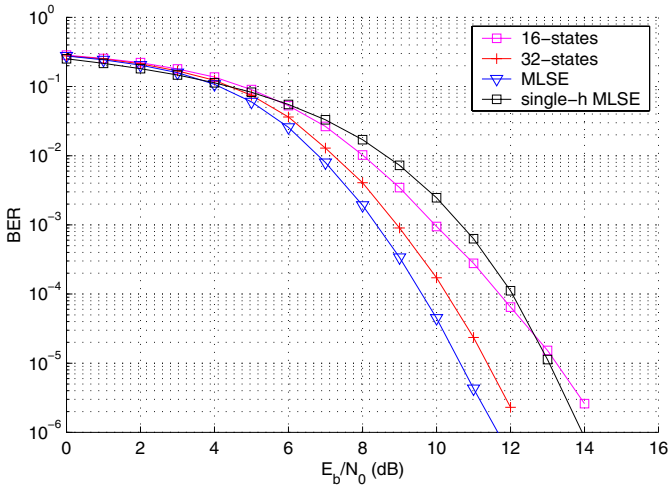

Fig. 6. Performance of 4-ary $3RC$ with $h = \{4/16, 5/16\}$. Simulations show 32-state receiver has a loss of 0.7 dB at BER $= 10^{-5}$. The 16-state receiver has a loss of 2.6 dB at the same BER. Multi-h performance gains are again preserved over a similar single-h scheme, $h = 1/4$, $M = 4$, and $L = 3RC$.

Quaternary $3RC$ with $h = \{4/16, 5/16\}$

The second scheme we consider is $M = 4$, $L = 3RC$, $h = \{4/16, 5/16\}$. This is the Advanced Range Telemetry (ARTM) Tier II proposed waveform [8]. Here we select two different approximation paths which yield receivers of comparable complexity, 16-states and 32-states, which is a dramatic reduction from the 512-state MLSE receiver. The first case is shown in Table IV on the left. Here we apply Approximation #1 to the degree proposed by Mengali [6] yielding $2 \cdot 3$ pulses and a 32 state trellis. We then average the pulses over the modulation indexes (Approximation #2) which reduces the number of matched filters to 3. We combine the two length-$3T$ pulses using Approximation #3, and finish by selecting $p' = 16$ to arrive at 2 matched filters and a 16-state trellis. Table IV also shows the cumulative loss of 2.6 dB these approximations incur with respect to MLSE at the operating point BER $= 10^{-5}$. Most of this loss is the result of Approximation #1.

The second case is shown in Table IV on the right. Here we apply Approximation #1 less aggressively, which results in $2 \cdot 12$ pulses and a 128-state trellis. We use Approximation #2 as before and Approximation #3 as shown in Figure 4, which yields 3 pulses, the trellis states unchanged, and a loss of 0.2 dB thus far. Approximation #4 reduces the trellis to 32 states with $p' = 8$ and an additional loss of 0.5 dB. By pursuing Approximation #1 less aggressively, the total loss is only 0.7 dB, an improvement of nearly 2 dB over the first case.

Performance curves for these receivers with respect to MLSE are shown in Figure 6. Also shown in the figure is the MLSE receiver for a single-h scheme, $h = 1/4$, $M = 4$, and $L = 3RC$, which requires 48 matched filters and a 128 state trellis. The figure shows that multi-h performance gains are largely preserved by the 32-state receiver, which is also significantly less complex than the single-h receiver (128 states, 48 matched filters).

VII. CONCLUSIONS

The multi-h CPM receivers presented in this paper are a viable alternative to the existing MLSE receiver for several reasons. First, the linear PAM decomposition is very flexible and allows many different possibilities for significant complexity reduction. We presented four specific approximations which reduce the number of matched filters and trellis states. The simulation results demonstrated that different combinations of these approximations produced very different results for a fixed level of complexity. The loss incurred by these approximations ranged from fractions of a dB to 2.6 dB for an extreme case.

Another advantage is that the approximations preserve the multi-h gain in the signal. This gain is often lost when using reduced-complexity receivers [1], [9]. An additional advantage is that they use a linear representation of the signal, and linear techniques can be applied to other receiver design problems such as synchronization.

REFERENCES

[1] J. B. Anderson, T. Aulin, C-E. Sundberg. *Digital Phase Modulation*. Plenum Press, New York, 1986.

[2] A. Svensson. "Reduced state sequence detection of partial responce continuous phase modulation". *IEE Proceedings, part I*, 138:256–268, August 1991.

[3] E. Perrins and M. Rice. "PAM decomposition of M-ary multi-h CPM". *submitted for publication in IEEE Transactions on Communications*.

[4] G. K. Kaleh. "Simple coherent receivers for partial response continuous phase modulation". *IEEE Journal on Selected Areas in Communications*, 7:1427–1436, December 1989.

[5] P. A. Laurent. "Exact and approximate construction of digital phase modulations by superposition of amplitude modulated pulses (AMP)". *IEEE Transactions on Communications*, 34:150–160, February 1986.

[6] U. Mengali and M. Morelli. "Decomposition of M-ary CPM signals into PAM waveforms". *IEEE Transactions on Information Theory*, 41:1265–1275, September 1995.

[7] Department of Defense Interface Standard MIL-STD-188-181B. "Interoperability standard for single-access 5-khz and 25-khz UHF satellite communications channels", 20 March 1999.

[8] M. Geoghegan. "Description and performance results for a multi-h CPM telemetry waveform". In *Proceedings of IEEE MILCOM*, volume 1, pages 353–357, October 2000.

[9] E. Perrins and M. Rice. "Comparison of receivers for multi-h CPM". In *Proceedings of the International Telemetering Conference*, San Diego, CA, October 2002.

[10] G. Colavolpe and R. Raheli. "Reduced-complexity detection and phase synchronization of CPM signals". *IEEE Transactions on Communications*, 45:1070–1079, September 1997.

[11] A. Ginesi, U. Mengali, and M. Morelli. "Symbol and superbaud timing recovery in multi-h continuous phase modulation". *IEEE Transactions on Communications*, 47:664–666, May 1999.

[12] L. Vandendorpe A. J. Rodrigues and A. A. Albuquerque. "Performance of direct-sequence spread spectrum multi-h CPM in indoor mobile radio systems". In *Proceedings of IEEE VTC'94*, June 1994.